Biochimica et Biophysica Acta, 464 (1977) 276—286

BBA 77574

TRANSPORT ACROSS EPITHELIA

A KINETIC EVALUATION

GENE BARNETT [a]* and VOJTECH LIČKO [b]

[a] *Deparment of Pharmaceutical Chemistry, School of Pharmacy and* [b] *Cardiovascular Research Institute, School of Medicine, University of California, San Francisco, Calif. 94143 (U.S.A.)*

(Received July 19th, 1976)

Summary

Compartmental analysis of three models for solute transport across epithelial tissue is presented. The simplest model describes only one tissue compartment, the second incorporates the notion of a pore as a parallel pathway and the third model introduces a serial compartment corresponding to non-epithelial portions of the tissue. Experimental data were obtained, using a modified Ussing and Zerahn technique ((1951) Acta Physiol. Scand. 23, 110—127), for salicylate transport across rat jejunum in vitro and analyzed in terms of these three models. The conclusions based solely on the mathematical analysis of this rather simple experiment are: the tissue is not a homogeneous penetration barrier as often considered. Transport is not limited by unstirred layers either at the tissue surfaces or within the tissue itself. Salicylate is not passively transported. Parallel transport pathways do exist.

Introduction

Various modifications of the method of Ussing and Zerahn [1] (Schultz and Zalusky [2]) have been extensively used in the past decade for the study of the transport of a variety of substances across tissues such as frog skin, toad bladder, mammalian intestine and mouse skin. Since this is an in vitro technique, the fluxes in either directions can be obtained. In general, one observes (Fig. 1) after a transient period, a linear rise of the concentration of substance transported through the tissue [3—7].

From these observations the steady-state flux of the substance is determined by the slope σ of the linear portion of the curve. The directional flux ratio so determined is a useful quantity to characterize the transport system. Another

* Present address: National Institute of Drug Abuse, Rockville, Md., U.S.A.

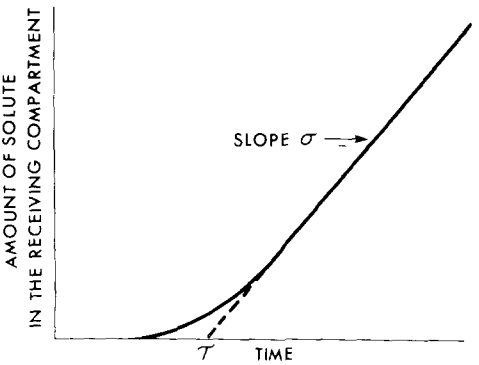

Fig. 1. Typical curve of solute transported into the receiving (sink) compartment with the slope of the linear portion σ (flux) and intercept of the extrapolated straight line τ (lag time).

observable quantity is the lag time τ. While a curve such as shown in Fig. 1 is usually described by the classical equation for diffusion applied to transport across a homogeneous barrier (cf. ref. 2) [8], we will show that such an equation has only limited validity.

A closer look at those curves which allow one to observe both the transient and the steady-state behavior suggests that there might be more parameters that one can determine, thus permitting a better understanding of the details involved in the absorption process. A compartmental approach seems to be a natural technique applicable to this end. In the following we review a number of simple models with which we analyze the experimental data reported here.

Compartmental models of absorption

(A) Model of tissue compartment

A schematic diagram of the model is shown in Fig. 2. In the diagram M represents the amount of the transporting solute in the mucosal bathing solution, S is the amount in the serosal solution and T is the amount of solute in the tissue. The Greek characters represent the corresponding rate coefficients, which are assumed constant, in units of time^{-1}. The system is defined in terms of linear differential equations as follows

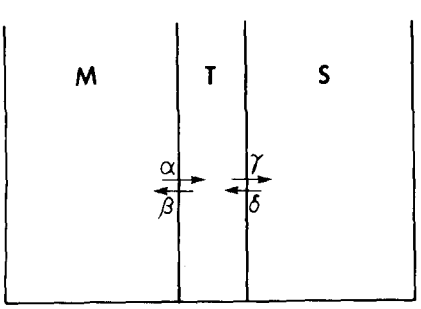

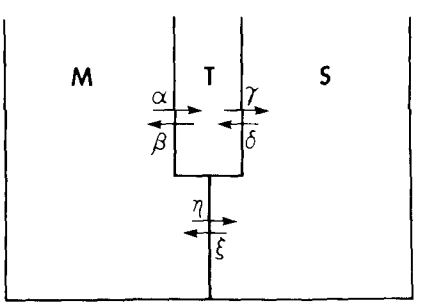

Fig. 2. Model A: Tissue (T) compartment. See text for detailed description.

Fig. 3. Model B: Tissue (T) with pore. See text for detailed description.

$$\dot{M} = -\alpha M + \beta T$$

$$\dot{T} = \alpha M - (\beta + \gamma)T + \delta S \tag{1}$$

$$\dot{S} = \gamma T - \delta S.$$

Experimentally the transport can be determined in either direction, thus, we have two sets of solutions to the equations and two sets of characteristic slopes and lag times for the two experimental curves. For transport from M to S, we define M as the source compartment and S as the sink compartment by setting $\dot{M} = 0$, $\delta S << \gamma T$. The amount of solute in the sink compartment S is then given by the traditional equation

$$S = \sigma_s(t - \tau_s) + \sigma_s\tau_s \exp(-t/\tau_s) \tag{2}$$

The flow into S is characterized by the slope σ_s and the lag time τ_s, viz.

$$\sigma_s = \frac{\alpha\gamma}{\beta + \gamma} \quad \text{and} \quad \tau_s = \frac{1}{\beta + \gamma} \tag{3}$$

Note that the exponential coefficient is precisely the reciprocal of τ_s. For transport in the reverse direction ($\dot{S} = 0$, $\alpha M << \beta T$) the increase as a function of time for the amount of solute M is

$$M = \sigma_m(t - \tau_m) + \sigma_m\tau_m \exp(-t/\tau_m) \tag{4}$$

The corresponding slope σ_m and lag time τ_m are

$$\sigma_m = \frac{\delta\beta}{\gamma + \beta} \quad \text{and} \quad \tau_m = \frac{1}{\gamma + \beta} \tag{5}$$

For this model then we find the ratio of slopes r_σ, the directional flux ratio, and the ratio of lag times r_τ are

$$r_\sigma = \frac{\alpha\gamma}{\delta\beta} \quad \text{and} \quad r_\tau = 1 \tag{6}$$

(B) Model of tissue with pore

The schematic diagram of this more complicated model is given in Fig. 3 where, in addition to the symbols of Fig. 1, the pore is characterized by the rate coefficients η and ξ. The kinetic equations are now

$$\dot{M} = -(\alpha + \eta)M + \beta T + \xi S$$

$$\dot{T} = \alpha M - (\beta + \gamma)T + \delta S \tag{7}$$

$$\dot{S} = \eta M + \gamma T - (\delta + \xi)S$$

For transport from M to S the assumed source and sink conditions are given by $\dot{M} = 0$, $\delta S << \gamma T$, $\xi S << \eta M$. The tradional equation no longer holds in its original form as the solute increase in S is now given by the following equation

$$S = \sigma_s(t - \tau_s) + \sigma_s\tau_s \exp[-(\beta + \gamma)t] \tag{8}$$

where the exponential coefficient $(\beta + \gamma)$ is not equal to the reciprocal of the lag time. In this model the slope and lag time are given by the following relations

$$\sigma_s = \frac{\alpha\gamma}{\beta + \gamma} + \eta \quad \text{and} \quad \tau_s = \frac{1}{\beta + \gamma} - \frac{\eta}{\eta(\beta + \gamma) + \alpha\gamma} \tag{9}$$

In these more complicated expressions for σ_s and τ_s we can identify the tissue and pore components since the first term in each case is the same expression that was obtained in model A (tissue only), Eqn. 3, while the second term is the contribution of the pore. We see that the introduction of a pore results in an additive contribution to the slope and a decrease in the lag time as compared to the previous model.

For transport in the opposite direction ($\dot{S} = 0$, $\alpha M << \beta T$, $\eta M << \xi S$) the expression for M is analogous to Eqn. 8 and the resulting slope and lag time are

$$\sigma_m = \frac{\delta\beta}{\gamma + \beta} + \xi \quad \text{and} \quad \tau_m = \frac{1}{\gamma + \beta} - \frac{\xi}{\xi(\gamma + \beta) + \delta\beta} \tag{10}$$

For this model the slope ratio and lag time ratio are considerably more complicated, viz.

$$r_\sigma = \frac{\alpha\gamma + \eta(\beta + \gamma)}{\delta\beta + \xi(\gamma + \beta)}$$

and

$$r_\tau = \frac{\alpha\gamma}{\delta\beta} \cdot \frac{\delta\beta + \xi(\gamma + \beta)}{\alpha\gamma + \eta(\beta + \gamma)} \tag{11}$$

(C) Model of epithelial and extraepithelial compartments with pore

The schematic diagram for the system is presented in Fig. 4. This model is an extension of model B (tissue with pore) by including an additional compartment X with exchange rate coefficients μ and ν. However, the interpretation is somewhat altered as E denotes only the epithelial cellular compartment and X denotes the extracellular compartment of the complete tissue. With this more extensive model the two-sidedness of the tissue is now more accurately represented. The general system of linear kinetic equations for this model is then

$$\begin{aligned} \dot{M} &= -(\alpha + \eta)M + \beta E + \xi X \\ \dot{E} &= \alpha M - (\beta + \gamma)E + \delta X \\ \dot{X} &= \eta M + \gamma E - (\delta + \xi + \mu)X \\ \dot{S} &= \mu X \end{aligned} \tag{12}$$

For the specific case of transport M to S the equations simplify slightly after introduction of the source and sink conditions ($\dot{M} = 0$, $\nu S << \mu X$), but the solution of these equations is still much more complicated than was the case of the previous models. Now there are two exponential terms in the function for S, describing the accumulation of solute, i.e.

$$S = \sigma_s(t - \tau_s) + \sigma_s[\tau_{s1}\exp(\lambda_1 t) + \tau_{s2}\exp(\lambda_2 t) \tag{13}$$

The slope σ_s of the straight line portion of the S curve is given by

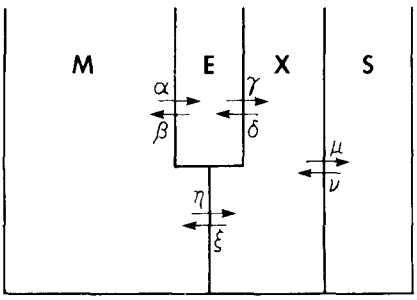

Fig. 4. Model C: Epithelial (E) and extraepithelial (X) compartments with pore. See text for detailed description.

$$\sigma_s = \left[\frac{\alpha\gamma}{\beta+\gamma} + \eta\right]\left[\frac{\mu(\beta+\gamma)}{(\beta+\gamma)(\delta+\xi+\mu)-\gamma\delta}\right] \tag{14}$$

and the lag time, which can be expressed as a sum, is

$$\tau_s = \tau_{s1} + \tau_{s2} = \frac{1}{\beta+\gamma}\left[\frac{(\beta+\gamma+\delta+\xi+\mu)(\beta+\gamma)}{(\delta+\xi+\mu)(\beta+\gamma)-\gamma\delta}\right] - \frac{\eta}{\eta(\beta+\gamma)+\alpha\gamma} \tag{15}$$

The components of τ_s are defines as

$$\tau_{s1} = \frac{\lambda_2}{\lambda_1-\lambda_2}\left[\frac{1}{\lambda_1} + \frac{\eta}{\eta(\beta+\gamma)+\alpha\gamma}\right]$$

and

$$\tau_{s2} = -\frac{\lambda_1}{\lambda_1-\lambda_2}\left[\frac{1}{\lambda_2} + \frac{\eta}{\eta(\beta+\gamma)+\alpha\gamma}\right] \tag{16}$$

where λ_1 and λ_2 are both real negative solutions to the characteristic equation corresponding to the system of differential equations, i.e. Eqn. 12 after source and sink conditions are introduced, viz.

$$\lambda^2 + (\beta+\gamma+\delta+\xi+\mu)\lambda + (\beta+\gamma)(\delta+\xi+\mu) - \gamma\delta = 0 \tag{17}$$

In this model, the expressions for the slope and lag time are, of course, even more complicated. Nevertheless, a similar separation of various components is obvious from Eqns. 9, 14 and 15. The slope σ_s has the tissue plus pore components which are now multiplied by a "shielding factor" due to the extracellular compartment X, which has the value less than unity (cf. the second factor in Eqn. 14). The lag time has a different "shielding factor" (again due to the X compartment) which modifies only the tissue component of τ_s (cf. the factor in brackets in Eqn. 15).

For transport in the reverse direction the solution to Eqn. 12 is again analogous to Eqn. 13 but the σ_s and τ_s are replaced by

$$\sigma_m = \left[\frac{\beta\delta}{\gamma+\beta} + \xi\right]\left[\frac{\nu(\gamma+\beta)}{(\delta+\xi+\mu)(\gamma+\beta)-\gamma\delta}\right] \tag{18}$$

and

$$\tau_m = \frac{1}{\gamma+\beta}\left[\frac{(\beta+\gamma+\delta+\xi+\mu)(\gamma+\beta)}{(\delta+\xi+\mu)(\gamma+\beta)-\gamma\delta}\right] - \frac{\xi}{\xi(\gamma+\beta)+\beta\delta} \tag{19}$$

In the formulas corresponding to τ_{m_1} and τ_{m_2} the last term in brackets in Eqn. 16 is replaced by the last term of Eqn. 19.

Simplification of model C. Various conditions for transport across epithelia may exist that introduce some simplification of model C and thus allow a better intuitive view of the transport system as described by this rather complicated model.

The solutions λ_1 and λ_2 of the characteristic equation, Eqn. 17, which appear as the exponential coefficients in Eqn. 13 are simplified if the condition holds that $\delta << (\xi + \mu)$, because then the term $\gamma\delta$ is negliglible. This would follow for a solute, passively transported, having a partition coefficient much different than unity where the lipid exit route from the extracellular compartment X is much slower than the two aqueous routes. Then

$$\lambda_1 \cong -(\beta + \gamma) \quad \text{and} \quad \lambda_2 \cong -(\xi + \mu) \tag{20}$$

where $S(t)$ is still a two-exponential function of course, and has a lag time, e.g. τ_s, given by

$$\tau_s \cong \frac{1}{\beta + \gamma} - \frac{\eta}{\eta(\beta + \gamma) + \alpha\gamma} + \frac{1}{\xi + \mu}. \tag{21}$$

This condition applies regardless of the relative magnitudes of λ_1 and λ_2, i.e. whether they are equal or different.

(a) Thick X compartment. The rate coefficients α, β, γ, δ, η, ξ, μ and ν can be expressed as AP/V where A is the tissue area across which transport occurs, P is the tissue permeability which can include both active and passive components, and V is the volume of the driving compartment. In the case of the extracellular compartment X, which is much larger than the epithelial compartment E, the respective volumes are $V_x >> V_e$. It then follows that since β and γ contain V_e in the denominator and ξ and μ are inversely proportional to V_x,

$$\beta + \gamma >> \xi + \mu$$

may hold and then from Eqn. 16

$$\tau_{s_1} \cong 0 \quad \text{and} \quad \tau_{s_2} \cong \frac{1}{\xi + \mu} \tag{22}$$

thus the function describing S will behave as a one-exponential function, Eqn. 2. As a consequence of this condition, X being a very large portion of the tissue, even if the tissue does have transport via a pore pathway as well as across the epithelial pathway the process is describable by model A (tissue with no pore) and the exponential coefficient characterizes only the extracellular compartment X and contains no information about the epithelial portion of the tissue.

(b) Thin X compartment. This is the opposite of the situation discussed in (a) as we now have $V_x << V_e$ and

$$\beta + \gamma << \xi + \mu$$

From inspection of Eqn. 16 under this condition it follows that

$$\tau_{s_1} \cong \frac{1}{\beta + \gamma} - \frac{\eta}{\eta(\beta + \gamma) + \alpha\gamma} \quad \text{and} \quad \tau_{s_2} \cong 0 \tag{23}$$

The solution for $S(t)$ is now given by Eqn. 8 as model B will describe the system in this case.

Experimental method

Salicylate flux across rat jejunum for serosal to mucosal and mucosal to serosal transport was measured by the technique of Ussing and Zerahn [1] as modified by Schultz and Zalusky [2]. The tissue chamber (E.W. Wright, Inc., New Haven, Conn.) consists of two half chambers with conical shape and 1.13 cm^2 cross-sectional area. Each half chamber was connected to a gas lift perfusion apparatus containing 10 ml of buffer solution and was heated to 37°C by water jackets. The composition of the buffer in mequiv/l was: 143.5 Na^+, 6 K^+, 2.4 Mg^{2+}, 5 Ca^{2+}, 128.3 Cl^-, 25 HCO_3^-, 1.2 $H_2PO_4^-$, 2.4 SO_4^{2-}, 25 glucose. The pH was adjusted to 7.4 with CO_2 and solution mixing was effected by the gas O_2/CO_2 (95 : 5, v/v). Sprague-Dawley male rats, weight 300—400 g, were killed by decapitation and four sections of tissue were excised from each animal for mounting on the cells by cutting along the mesenteric line from the segment of intestine 25—50 cm distal to the stomach. [^{14}C]Salicylic acid, 2 μCi and 0.1 mM, was introduced on one side of the tissue at 25 ± 5 min after death and the concentration was measured as a function of time on the other side.

Results

In Table I we present the characteristic slopes σ_s and σ_m (fluxes) and the lag times τ_s and τ_m, the index refering to the receiving (measured) side of the tissue. The data presented here were obtained by a linear least squares fit of the measurements taken at 10-min intervals from 20 min to 50 or 60 min after the label was introduced. The ratio of fluxes is 1.46 which is significantly different from unity at a level of $P < 0.0005$. This flux ratio is typical of values found for other weak electrolyte anion flux across rat jejunum [5,6]. However, the lag times are usually not reported. The ratio of lag times in our observations is 1.02, not significantly different from unity.

In order to evaluate the applicability of the models discussed above, some of the data were used for a more extensive mathematical analysis of the system. These data are presented in Table II where from the linear analysis of fluxes and lag times it appears that we have a representative subset of the complete data of Table I.

TABLE I

FLUXES AND LAG TIMES FOR RAT JEJUNUM

Flux (σ) is in units of nmol · cm^{-2} · min^{-1}. Lag time (τ) is in units of min.

	Mean	S.D.	Nos. of tissues
σ_s	0.084	0.032	35
σ_m	0.058	0.027	33
τ_s	13.9	2.1	33
τ_m	13.6	4.8	31

TABLE II

COMPARISON OF LINEAR AND NON-LINEAR FITTINGS IN A SUBSET OF EXPERIMENTAL DATA FROM TABLE I

Units for flux and lag time are given in Table I. Coefficient λ is in units of min^{-1}.

	Linear		Non-linear *		Nos. of tissues
	Mean	S.D.	Mean	S.D.	
σ_s	0.082	0.020	0.100	0.018	8
σ_m	0.067	0.022	0.075	0.019	5
τ_s	13.6	1.5	22.2	6.2	8
τ_m	13.4	2.0	19.5	5.2	5
$1/\lambda_s$	—	—	19.4	6.1	8
$1/\lambda_m$	—	—	17.8	4.1	5

* By model B.

In an effort to fully characterize the transport system we have analyzed the experiments reported in Table II by a non-linear least squares analysis BMD07R (Dixon, cf. 9) based on model C, that of epithelial and extraepithelial compartments with pore. The experimental data were obtained by measurements at 5-min intervals from the time the label was introduced until 20 min and then at 10-min intervals until 60 min. Utilizing Eqn. 13, we attempted to obtain estimates for the five parameters, namely $\sigma, \tau_1, \tau_2, \lambda_1, \lambda_2$ (note that $\tau = \tau_1 + \tau_2$ cf. Eqn. 15). This effort was not successful: either the process did not converge and/or the standard deviations of the parameter estimates rendered them useless. However, we did carry out the analysis within the framework of model B, that of tissue with pore. The non-linear portion of Table II was obtained in this manner. In the table, λ represents the experimental parameter which in Eqn. 8 is defined as $\beta + \gamma$.

Under closer examination of the parameters obtained (σ, τ and $1/\lambda$) by the non-linear fitting of model B to the experimental data we see that τ is always greater than $1/\lambda$. For transport from M to S the difference between τ_s and $1/\lambda_s$ by a paired t-test is highly significant: $P << 0.0005$. For transport in the opposite direction, the difference between τ_m and $1/\lambda_m$ was significant at the level of $0.025 < p < 0.05$. Since model A is a special case of model B, i.e. no pore ($\eta = \xi = 0$), this analysis covered that case as well.

Discussion

In the analysis by model B reported in Table II the difference between τ and $1/\lambda$ which was significant, forces us to exclude model A as a valid model for this system since, according to Eqns. 2 and 3, $\tau = 1/\lambda = 1/(\beta + \gamma)$. Furthermore, the observation that $\tau > 1/\lambda$ forces us to exclude model B since, according to Eqns. 9 and 10 τ must be less than $1/\lambda = 1/(\beta + \gamma)$. Therefore, while neither model A nor model B is satisfactory, we would like to investigate the possibility that model C is in fact a valid description of this system.

In an effort to resolve the difficulty of not being able to analyze the experimental data by model C we have carried out a series of digital simulations of experiments utilizing Eqn. 13, generating curves $S(t)$ similar to Fig. 1 by intro-

ducing a normal scatter into the computed data. For these simulations we have chosen values of α, β, γ, δ, η, ξ, μ and ν, non-negative parameters, such that σ and τ would be characteristic of the observed values by linear or non-linear analyses (i.e. $\sigma \cong 0.1$ nmol $\cdot$ cm^{-2} $\cdot$ min^{-1} and $\tau \cong 15$ min). Obviously there is no unique solution to this problem but through extensive searching we can classify two types of solutions, namely such that $\lambda_1 >> \lambda_2$ or the $\lambda_1 \approx \lambda_2$. These two classes of solutions can be exemplified by the two sets of parameters included in Table III *.

When the simulated data with 0% standard deviation of the normal scatter were analyzed by model C, only in the case of $\lambda_1 \approx \lambda_2$ could we recover the "experimental" parameters used for data generation. Using scattered data with 5% standard deviation no fitting was obtained. This was also the case with our efforts reported above to attempt an analysis of the experimental data in Table II by model C. Clearly, the curves obtained by the type of experiment reported here do not contain sufficient information to allow one to estimate the experimental parameters for model C.

Nevertheless, the analysis by model B of the data generated by simulation of model C (shown in Table IV) was carried out more successfully. For each case reported in Table IV, the values are the averages of five simulations with data scattered at the 5% standard deviation level. In the case of $\lambda_1 >> \lambda_2$, we found that $\tau_s < 1/\lambda_s$ which was statistically significant at the level of $P < 0.005$. This is in contradiction to the results of the analysis of experimental data as reported in Table II. However, the analysis of the case $\lambda_1 \cong \lambda_2 (\lambda_1 \geqslant \lambda_2)$ we

TABLE III

TWO EXAMPLES OF VALUES OF MODEL PARAMETERS AND "SIMULATED EXPERIMENTAL" PARAMETERS OF MODEL C LEADING TO $\sigma_s = 0.1$ nmol $\cdot$ cm^{-2} $\cdot$ min^{-1} and $\tau_s = 15$ min

Model parameters are in units of min^{-1}. For units of "Simulated experimental" parameters see Table II.

Parameters	$\lambda_1 >> \lambda_2$	$\lambda_1 \approx \lambda_2$
Model		
α	$0.15 \cdot 10^{-3}$	$0.16 \cdot 10^{-3}$
β	$0.3 \cdot 10^{-1}$	0.12
γ	$0.3 \cdot 10^{-1}$	0.13
δ	$0.3 \cdot 10^{-1}$	$0.175 \cdot 10^{-1}$
η	$0.15 \cdot 10^{-4}$	$0.36 \cdot 10^{-4}$
ξ	$0.3 \cdot 10^{-2}$	$0.55 \cdot 10^{-2}$
μ	3.0	$0.65 \cdot 10^{-1}$
ν	$0.15 \cdot 10^{-1}$	$0.28 \cdot 10^{-3}$
"Simulated experimental"		
σ_s	0.0895	0.0982
τ_{s1}	14.25	16.96
τ_{s2}	0.0491	−1.035
τ_s	14.30	15.93
λ_{s1}	−0.0597	−0.075
λ_{s2}	−3.0333	−0.263

* By restricting the parameters further to simulate a passive transport model we arrived at the solution of the type $\lambda_1 >> \lambda_2$. As will be seen below, this is not a valid description of the system.

TABLE IV

ESTIMATES OF "SIMULATED EXPERIMENTAL" PARAMETERS BY FITTING SIMULATED CURVES WITH MODEL PARAMETERS OF TABLE III TO MODEL B

For units see Table II.

	$\lambda_1 >> \lambda_2$	$\lambda_1 \cong \lambda_2$
σ_s	0.0898 ± 0.0079	0.1061 ± 0.0061
τ_s	14.6 ± 3.4	19.1 ± 2.3
$1/\lambda_s$	17.0 ± 4.6	13.0 ± 2.8

found that $\tau_s > 1/\lambda_s$ at the level of significance $P < 0.005$. This observation is fully compatible with the results of our non-linear analysis of the experimental data (Table II) using the functional form of model B as a device to test the data for compatibility with models A and B. As mentioned above, the observation that $\tau_s \neq 1/\lambda_s$ allows us to exclude model A as a valid description of this system. Furthermore, as noted above, the fact that $\tau_s > 1/\lambda_s$ allows us to exclude model B as well. Therefore, on the basis of these observations, we conclude that model C is the minimal compatible model that may be appropriate for a description of this system of intestinal anion transport.

This type of analysis has also been applied to the transport of methotrexate across mouse skin where model B was found appropriate to describe the system and to rationalize the pH dependence of solute flux. [10].

Conclusions

Due to the mathematical nature of the foregoing analysis we enunciate our conclusions and related implications in detail here. We wish to stress that these findings are based solely on the mathematical analysis of the experiment and therefore stand as independent evidence to those biochemical and physicochemical studies which lead to similar conclusions.

(1) The tissue is not a homogeneous barrier to solute transport. This follows from our finding that model A is not a valid description for the sytem of salicylate transport across rat jejunum. As a consequence, analysis via the classical diffusion equation [8], which forces the system to obey model A, does not extract complete information when applied to this type of experiment.

(2) Transport is not rate limited by unstirred layers either at the tissue surfaces or within the tissue. This type of process would be described by model A. While we have suggested that model C may be appropriate, the considerations leading to Eqn. 22 make it clear that the X compartment is not "thick" as that would again lead back to an A type model.

(3) Multiple transport pathways exist for this system. The finding that model C is the simplest possible description of the tissue requires that there are at least parallel transport pathways.

(4) Salicylic acid is not passively transported. The simulation studies could not reproduce the experimental observations when the parameters were restricted to obey a passive model.

Clearly this type of analysis stands self-justified in view of these results. To

make these observations directly would require a considerable amount of experimentation beyond the rather simple procedure applied here. The value of the compartmental analysis is further enhanced as it suggests a more complete definition of the experiment (and tissue) through additional measurements that would be desirable. In particular, it is advantageous to do flux measurements in both directions across the tissue. Measurements of the amount of solute in the tissue, especially as a function of time, would allow further definition of the parameters. If techniques to determine cellular and extracellular amounts as a function of time were developed it could then allow one to obtain all the parameters introduced by model C. Finally, this type of analysis has a broad applicability to many experimental tissue and solute systems.

Acknowledgements

This work was supported by N.I.H. Grant GM 16496 to Professor L.Z. Benet in whose laboratory the experimental work was performed.

References

1 Ussing, H. and Zerahn, K. (1951) Acta Physiol. Scand. 23, 110–127
2 Schultz, S. and Zalusky, R. (1964) J. Gen. Physiol. 47, 567–584
3 Quay, J. and Armstrong, W. (1969) Am. J. Physiol. 217, 694–702
4 Field, M., Fromm, D. and McColl, L (1971) Am. J. Physiol. 220, 1388–1396
5 Jackson, M., Shiau, Y., Bane, S. and Fox, M. (1974) J. Gen. Physiol. 63, 187–213
6 Barnett, G., Hui, S. and Benet, L. (1976) Submitted to Am. J. Physiol
7 Wallace, S., Runikis, J. and Stewart, W. (1976) J. Pharm. Pharmacol., in the press
8 Jost, W. (1952) Diffusion in Solids, Liquids and Gases, p. 37, Academic Press, New York
9 Dixon, W. (1974) BMD Biomedical Computer Programs, University California Press, Berkeley
10 Walace, S., Barnett, G. and Licko, B. (1976) Submitted to J. Pharmacokin. Biopharm.